COBEM 2023 27TH INTERNATIONAL CONGRESS OF MECHANICAL ENGENEERING

ABCM Brazilian Society of Mechanical Sciences and Engineering
27th ABCM International Congress of Mechanical Engineering
December 04-08, 2023, Florianópolis-SC, Brazil

COB-2023-1592
MACHINE LEARNING-BASED REDUCED-ORDER MODELS FOR BURGERS AND SHALLOW-WATER EQUATIONS

Pedro Roberto Barbosa Rocha
Marcos Sebastião de Paula Gomes
Department of Mechanical Engineering, Catholic University of Rio de Janeiro, PUC-Rio, 22451-900, Rio de Janeiro, RJ, Brazil
prbarbosr@gmail.com, mspgomes@puc-rio.br

Abstract. *Scientific machine learning methods that incorporate physics knowledge on a data-driven learning have become quite promising for the representation and prediction of nonlinear fluid flow systems with multiple scales in space and time. This work addresses one of these methods, the Operator Inference (OpInf), in the context of model order reduction. By solving a multivariable regression problem in latent space, the OpInf seeks for optimal low-dimensional operators that represent the system dynamics. Its capabilities are illustrated throughout this paper and compared with popular machine learning frameworks found in literature, such as physics-informed neural networks (PINNs), Fourier neural operators (FNOs) and auto-encoding neural networks (U-Nets). Two representative cases with known physical parameters were evaluated: Burgers and shallow-water equations. The predictive performance of the reduced-order model (ROM) was assessed for each case and normalized root-mean-square errors were computed for the state variables of interest. For instance, they were below 6.2% for the dependent variable of the Burgers equation at the middle of the one-dimensional domain. Moreover, OpInf-based models require much less training time than neural networks since they have a small number of hyperparameters to be tuned. While here the ROM for the shallow-water equations took 25 seconds to be trained, it was recently reported in literature that more than 10 minutes were required to train a PINN-based surrogate model using the same training dataset. All these features highlight the great potential of the non-intrusive operator inference framework for model order reduction of fluid flow systems.*

Keywords: *scientific machine learning, model order reduction, fluid dynamics*

1. INTRODUCTION

With the increasing availability of data provided by real-world applications, high-fidelity multiscale numerical simulations and laboratory experiments, data-driven machine learning (ML) algorithms have emerged as an effective way of generating more insights and knowledge about the related dynamical systems, improving decision-making processes. In the fields of climate and thermal sciences and fluid dynamics, one may be interested in obtaining a surrogate model capable of representing a physical system and estimating its future states given initial and boundary conditions and, possibly, some constraints. However, the associated dataset, which contains parameter-dependent spatiotemporal fields, is often quite large due to the necessity of a higher resolution to capture relevant small scale phenomena. This fact imposes a great challenge to the ML algorithm, that will learn the system and be able to perform future state predictions.

The main ML-based alternatives to address this surrogate modeling involve deep learning models (Lui and Wolf, 2019), physics-informed neural networks (PINNs) (Raissi et al., 2019) and operator learning frameworks (OLFs) (Lu et al., 2021; Qian et al., 2022). Among the OLFs, there are the dynamic mode decomposition (DMD) (Schmid, 2010), deep operator networks (DeepONets) (Lu et al., 2021), Fourier neural operators (Kovachki et al., 2021), sparse identification of nonlinear dynamical systems (SINDy) (Brunton et al., 2016) and the non-intrusive operator inference (OpInf) (Peherstorfer and Willcox, 2016). These techniques are capable of determining the main features of a dynamical system in order to have a better insight about the underlying physical phenomenon. Furthermore, they may be employed to build reduced-order models (ROMs), a simplification of complex ones. These reduced models are quite important when dealing with shorter design cycles, digital twins and larger systems simulations and also with optimization, uncertainty quantification and inverse problems.

To build ROMs for unsteady flows, Eivazi et al. (2020) combined an autoencoder for nonlinear dimensionality reduction with a long short-term memory (LSTM) artificial neural network (ANN). With this autoencoder-LSTM model, it was possible to predict velocity fields beyond the training horizon, considering as test cases the flow around a cylinder and a NACA0012 airfoil. The number of layers, the number of neurons within the hidden layers and the activation function of both neural networks were the hyperparameters of the model, whose tuning was quite computationally expensive. Besides, Wang et al. (2019) developed non-intrusive reduced-order models for unsteady flows using proper orthogonal decomposition (POD) and ANNs. Temporal, physical and geometrical parameters were the input of the feedforward neural network, while the POD coefficients were the output. The authors observed that interpolation techniques might fail if only a small number of training samples were available. So, a significant amount of data is required to train this

kind of model. Also, Wang et al. (2019) highlighted three hours were necessary to decompose the high-fidelity solutions and train the ANN with no hyperparameters optimization. Differently than the aforementioned authors, Yu and Hesthaven (2022) built intrusive projection-based ROMs for compressible flows, taking into account the weak and the strong forms of the discontinuous Galerkin method. They employ methods to enhance stability of the ROM, a challenge shared among projection-based methods.

The OpInf method seeks for linear and nonlinear operators that represent a dynamical system in a latent space, whose basis is obtained through a proper orthogonal decomposition (POD) of the respective high-fidelity dataset. This method is data-driven, i.e., the reduced model is built from spatiotemporal data gathered from experiments or numerical simulations. Although being data-driven, an OpInf-based ROM incorporates the system's physical information, which is a quite positive aspect in comparison with black-box ML techniques. Also, it is non-intrusive, meaning one does not need access to the high-fidelity operators embedded in the governing partial differential equations (PDEs). The OpInf has been successfully applied in combustion problems (McQuarrie et al., 2021), chaotic systems (Almeida et al., 2022), atmospheric CO_2 dispersion (Rocha et al., 2022) and natural convection (Rocha et al., 2023).

In this work, reduced-order models for two fluid flow systems described by Burgers and shallow-water equations were obtained through the non-intrusive operator inference method. The model performance was compared with literature in terms of computational efficiency and predictive accuracy. For that, results from PINNs, FNOs and auto-encoding neural networks (U-Nets) were considered. In summary, the following procedure was followed: (1) high-fidelity datasets (i.e., the spatiotemporal data corresponding to the numerical solution of the governing equations) for the dynamical systems of interest were gathered from literature; (2) the dimensionality of these datasets was reduced via proper orthogonal decomposition and (3) a multivariable regression problem with regularization was solved in latent space. The paper is divided into 5 main sections. Section 2 briefly describes the governing equations of the full-order models (FOMs) and the numerical methods applied in the literature to solve them. Section 3 presents an overview of the OpInf method. Section 4 discusses the main results achieved by the OpInf-based ROMs for Burgers and shallow-water equations and Section 5 concludes the paper.

2. FULL-ORDER MODELING

The high-fidelity numerical solutions for the Burgers and shallow-water equations were obtained from PDEBENCH (Takamoto et al., 2023), a collection of benchmark datasets generated from time-dependent numerical simulations of a variety of fluid flow systems. This benchmark suite was chosen since it allows the comparison of scientific ML methods, such as the OpInf, with classical numerical simulations and baseline (or reference) ML models. Here, FNOs, PINNs and U-Nets were the reference models against which OpInf was compared.

2.1 Burgers equation

The Burgers' equation is a nonlinear PDE that models convection and diffusion processes in fluid dynamics and other research areas. For a one-dimensional (1D) domain, it may be written as

$$\frac{\partial u}{\partial t} + u\frac{\partial u}{\partial x} = \nu\frac{\partial^2 u}{\partial x^2}, \tag{1}$$

where $u = u(x,t)$ is the dependent field variable of the Burgers' equation, ν is the kinematic viscosity (i.e., the diffusion coefficient), $x \in (0,1)$ and $t \in (0,2]$. Takamoto et al. (2023) considered periodic boundary conditions and a superposition of sinusoidal waves as the initial condition. The authors employed a second-order upwind difference scheme for the advection term and a central difference scheme for the diffusion term. In the present work, it was selected the dataset in which $\nu = 0.01$. Besides, the field variable was computed in 1,024 grid points over 200 time instants.

2.2 Shallow-water equations

These hyperbolic PDEs model free surface flows. In a two-dimensional (2D) setting, they may be written as

$$\frac{\partial h}{\partial t} + \frac{\partial (hu)}{\partial x} + \frac{\partial (hv)}{\partial y} = 0\,, \tag{2a}$$

$$\frac{\partial (hu)}{\partial t} + \frac{\partial}{\partial x}\left(u^2 h + \frac{1}{2}g_r h^2\right) + \frac{\partial (uvh)}{\partial y} = -g_r h\frac{\partial b}{\partial x}, \tag{2b}$$

$$\frac{\partial (hv)}{\partial t} + \frac{\partial}{\partial y}\left(v^2 h + \frac{1}{2}g_r h^2\right) + \frac{\partial (uvh)}{\partial x} = -g_r h\frac{\partial b}{\partial y}, \tag{2c}$$

where u and v are the velocities in x (horizontal) and y (vertical) directions, h is the water depth, b is the spatially varying bathymetry, hu and hv represent directional momentum components and g_r is the acceleration due to gravity.

Takamoto et al. (2023) explored a 2D radial dam break scenario on a square domain $\Omega = [-2.5, 2.5]^2$ with 128 grid points in each direction. For this case, 100 snapshots (or time instants) were stored. They considered the initial water depth as a circular bump with radius r, whose center was placed at $(x, y) = (0, 0)$. The value for r was randomly sampled from the interval $[0.3, 0.7]$. More details about the numerical methods implemented to solve Eqs. (2a-2c) were discussed by Takamoto et al. (2023).

3. REDUCED-ORDER MODELING

The non-intrusive operator inference (OpInf) is a scientific machine learning approach that blends data-driven learning with physics-based modeling. Initially, we have a system of PDEs corresponding to the physics-based model, which may be linear or not. The projection-based reduced model, that lies in a low-dimensional subspace, has the same structured form of the physics-based model. With no forcing term, we have:

$$\frac{d}{dt}\widehat{\mathbf{q}}(t) = \widehat{\mathbf{c}} + \widehat{\mathbf{A}}\widehat{\mathbf{q}}(t) + \widehat{\mathbf{H}}(\widehat{\mathbf{q}}(t) \otimes \widehat{\mathbf{q}}(t)) , \tag{3}$$

in which vector and matrix quantities are represented in bold, $\widehat{\mathbf{q}}(t)$ are the time-dependent latent field variables and $\widehat{\mathbf{c}}$, $\widehat{\mathbf{A}}$ and $\widehat{\mathbf{H}}$ are the low-dimensional operators to be computed through a multivariable regression problem with regularization to avoid overfitting. The OpInf framework is detailed next.

3.1 Collection of physical data

Initially, high-fidelity spatiotemporal data ($\mathbf{q}(t)$) are gathered from experiments, numerical simulations or real-world measurements. Then, the original data matrix $\mathbf{D} \in \mathbb{R}^{k \times n}$ is assembled, where $\mathbf{q}(t)$ are the rows of $\mathbf{D}$, k is the number of training snapshots (or time instants) and n is the number of degrees of freedom. For instance, if there were 100 grid points and 2 field variables of interest (e.g., pressure and x-velocity), n would be equal to 2 x 100 = 200 degrees of freedom.

3.2 Dimensionality reduction

To reduce data dimensionality, the principal component analysis (PCA) algorithm from Scikit-learn (Pedregosa et al., 2011) was employed. It is a POD technique (Weiss, 2019) based on the singular value decomposition (SVD) of the data, representing them in a lower-dimensional subspace (a.k.a. latent space). Thus, the original data matrix $\mathbf{D}$ may be written as

$$\mathbf{D} = \mathbf{U}\boldsymbol{\Sigma}\mathbf{V}^{\mathbf{T}} , \tag{4}$$

with $\mathbf{U} \in \mathbb{R}^{k \times k}$ and $\mathbf{V} \in \mathbb{R}^{n \times n}$ portraying the left and right singular vectors of $\mathbf{D}$ and $\boldsymbol{\Sigma} \in \mathbb{R}^{k \times n}$ being a diagonal matrix with the singular values of $\mathbf{D}$, σ_i, in a decreasing order. The r columns of $\mathbf{V}$, $\mathbf{V}_r$, whose associated singular values are the highest, are the POD basis onto which $\mathbf{D}$ is projected, obtaining $\mathbf{D}_r$ ($\mathbf{D}_r = \mathbf{D}\mathbf{V}_r$). Thus, data dimensionality is reduced from n to $r \ll n$. Note that $\widehat{\mathbf{q}}(t)$, the latent field variables, are the rows of $\mathbf{D}_r$. To select an adequate value for r, an energetic criterion was applied. For that, the ratio $\sum_{i=1}^{r} \sigma_i \,/\, \sum_{i=1}^{n} \sigma_i$ was computed. More features of the dynamical system are captured as this ratio approaches 1.

3.3 Multivariable regression with regularization

After computing numerically the left-hand side of Eq. (3), which may also be written as $\dot{\widehat{\mathbf{q}}}_i$ with the dot indicating time derivative, the multivariable least-squares regression problem with regularization becomes

$$\min_{\widehat{\mathbf{c}},\widehat{\mathbf{A}},\widehat{\mathbf{H}}} \left\{ \sum_{i=0}^{k-1} \left\| \widehat{\mathbf{c}} + \widehat{\mathbf{A}}\widehat{\mathbf{q}}_i + \widehat{\mathbf{H}}(\widehat{\mathbf{q}}_i \otimes \widehat{\mathbf{q}}_i) - \dot{\widehat{\mathbf{q}}}_i \right\|_2^2 + \lambda_1 \left(\|\widehat{\mathbf{c}}\|_2^2 + \left\|\widehat{\mathbf{A}}\right\|_F^2 \right) + \lambda_2 \left\|\widehat{\mathbf{H}}\right\|_F^2 \right\},$$

where λ_1 and λ_2 are the regularizers that penalize each entry of the operators $\widehat{\mathbf{c}}$, $\widehat{\mathbf{A}}$ and $\widehat{\mathbf{H}}$. Both are the model hyperparameters to be tuned through the following three-step process: (i) with tentative λ_1 and λ_2, the regression problem is solved and $\widehat{\mathbf{c}}$, $\widehat{\mathbf{A}}$ and $\widehat{\mathbf{H}}$ are determined; (ii) the ROM, described by Eq. (3), is integrated over time from the initial condition and (iii) the integration error is computed. This process is repeated until a minimum error is reached.

3.4 Error evaluation

The integrated reduced variables, $\tilde{\mathbf{q}}(t)$, are projected back onto the original space by multiplying them by $\mathbf{V}_r^T$, resulting in $\mathbf{q_{rec}}(t)$. Note that $\tilde{\mathbf{q}}(t)$ were obtained for optimal regularizers. The recovered (or approximated) variables, $\mathbf{q_{rec}}(t)$ are compared with the original ones, $\mathbf{q}(t)$. Also, let s_i and s_i^{rec} be the original and recovered state variables of interest at a probe location, where $s \in \{u, h\}$ (u for the Burgers and h for the shallow-water case) and the subscript i indicates the time step. The normalized root-mean-square ROM error along a given interval at the same location, ϵ_{rom}, is given by

$$\epsilon_{rom} = \frac{1}{\Delta S}\sqrt{\frac{\sum_{i=1}^{N}(s_i - s_i^{rec})^2}{N}}, \tag{5}$$

where $\Delta S = \max\{s_i\} - \min\{s_i\}$, $i = 1, 2, 3, \ldots, N$, is the maximum variation of the variable s at the probe location. Also, N refers to the number of training or testing snapshots. If one wishes to compute the error along the training interval, N should be the number of training snapshots.

4. RESULTS AND DISCUSSION

The OpInf framework was applied for two unsteady fluid dynamics problems, one described by the 1D Burgers formulation and another by the 2D shallow-water equations. In this section, ROM outputs are properly analyzed and compared with the original high-fidelity fields to assess model's accuracy, efficiency and robustness, both globally and locally. It is worth mentioning that the same software architecture was employed for both cases. The main differences are on the general setup of the OpInf framework, which is presented in Table 1.

Table 1. General setup of the OpInf framework.

Parameters	**1D Burgers**	**2D shallow-water**
Simulation time step	0.01	0.01s
Number of latent field variables (r)	4	10
Number of training snapshots (k_{train})	120	90
Number of testing snapshots (k_{test})	80	10

4.1 Case 1: 1D Burgers equation

The exact latent field variables, $\hat{\mathbf{q}}(t)$, obtained after projecting the simulation data onto the POD basis, and those approximated by the ROM, $\tilde{\mathbf{q}}(t)$, were compared. The smaller the difference between $\tilde{\mathbf{q}}(t)$ and $\hat{\mathbf{q}}(t)$, the more accurate the reduced model is. Although the ROM may be precise throughout the training interval, its robustness to time integration beyond that is not guaranteed *a priori*. To check that, the exact and approximated four most energetic latent field (or reduced) variables are exhibited in Figure 1. Note that the ROM integration starts at the initial time instant and remains quite robust and accurate even beyond the training interval, which demonstrates its effectiveness for temporal extrapolation. Furthermore, only 60% of the high-fidelity data was used to train the model, showing the method does not depend on a very high number of training snapshots as standard neural networks.

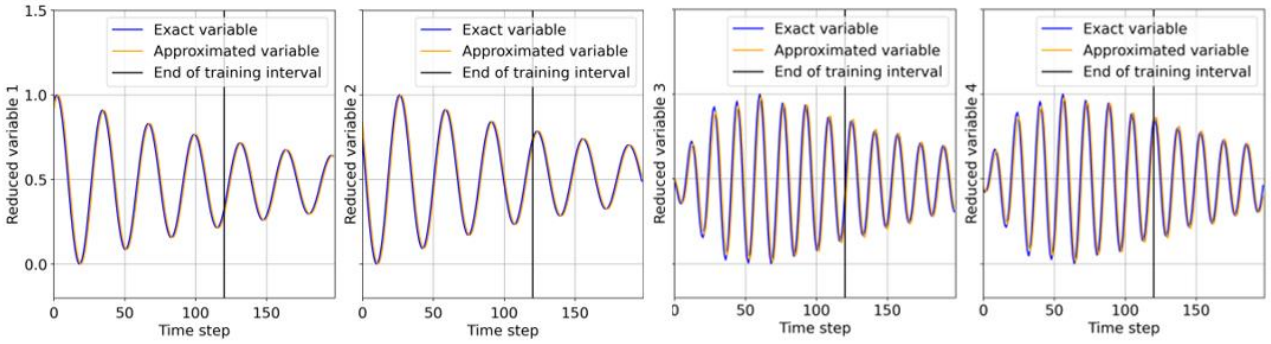

Figure 1. Temporal evolution of the exact and approximated four most energetic reduced variables for case 1.

The spatiotemporal distribution of the dependent field variable of the Burgers' equation is depicted in Figure 2. There is a great correspondence between FOM and ROM outputs, with a maximum absolute error of about 0.015. Taking into

account that maximum and minimum values for the main variable are close to 0.83 and 0.72, respectively, this error is quite acceptable. Normalized root-mean-square ROM errors at the middle of the 1D domain, ϵ_{rom}, were computed. For the training region, $\epsilon_{rom} = 0.062$. For the testing one, $\epsilon_{rom} = 0.037$. The greater error along the training interval may be justified by higher oscillation amplitudes imposing more difficulties for numerical integration. The results also indicate the efficiency of the OpInf-based model.

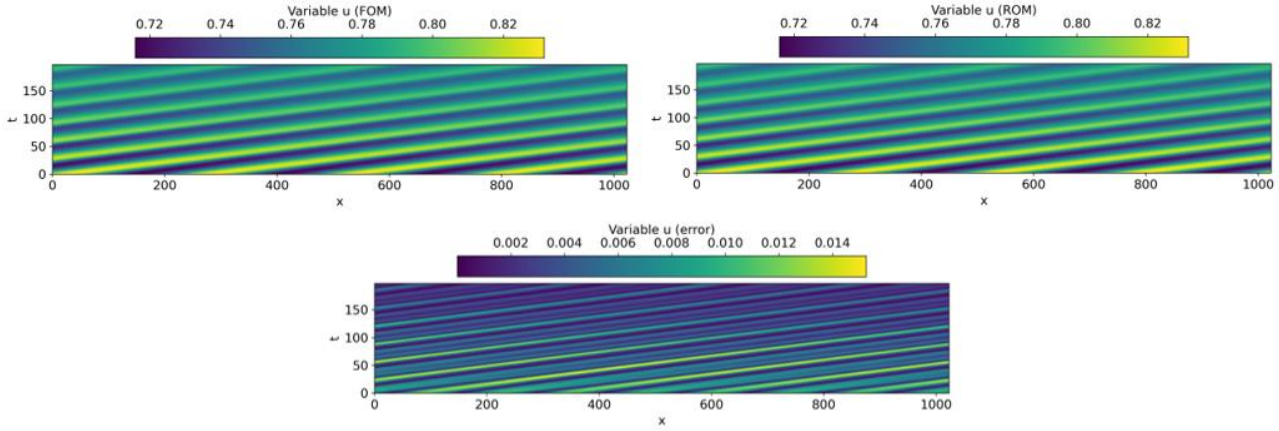

Figure 2. Spatiotemporal distribution of the dependent field variable of the Burgers' equation.

4.2 Case 2: 2D shallow-water equations

Similarly to the previous analyses, the four most energetic reduced variables are presented in Figure 3. However, for the shallow-water case, 90% of the high-fidelity data was used to train the model due to a greater complexity of the dynamical system and a lack of representative snapshots - only 100 of them were simulated by Takamoto et al. (2023). In spite of that, the ROM was capable of providing good approximations for both training and testing regions.

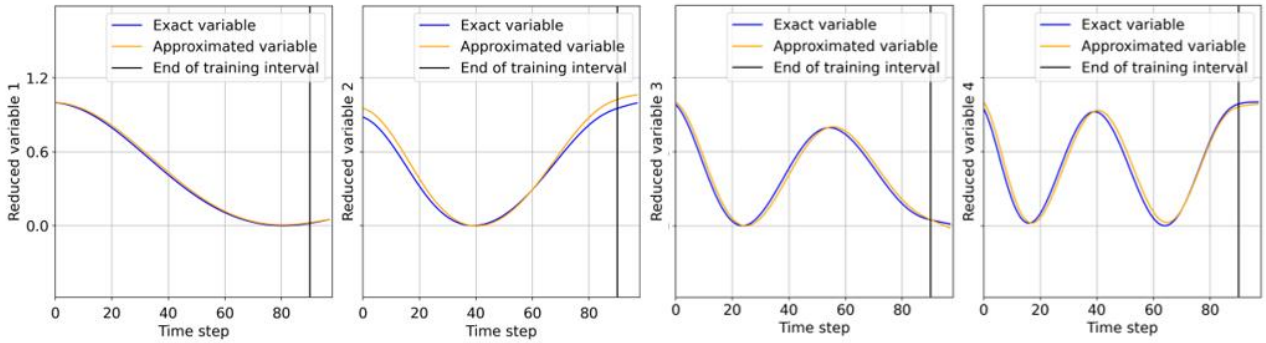

Figure 3. Temporal evolution of the exact and approximated four most energetic reduced variables for case 2.

The spatial distribution of the water depth h at the last training snapshot is represented in Figure 4. It may be seen the transition between different depths is less smooth in the ROM, a fact justified by the substantial reduction in data dimensionality, from $128 \times 128 = 16{,}384$ degrees of freedom to $r = 10$ reduced variables. Furthermore, the maximum absolute error for the depth at the last training snapshot was about 0.14 m, which is also quite acceptable due to the values this variable assumes across the domain, from 0.2 to 1.2 m, approximately. With respect to the normalized root-mean-square ROM errors at the middle of the domain, they were equal to 2.2% for the training region and 8.3% for the testing one, showing the good accuracy of the reduced model.

4.3 Computational costs

The OpInf framework (including dimensionality reduction, multivariable regression with regularization and data reconstruction) was executed in a Mac Book Pro with a 2 GHz Intel Core i5 Quad-Core processor. For the shallow-water case, this execution took about 25 seconds. Takamoto et al. (2023) reported they have employed one NVIDIA Volta V100 GPU to build surrogate models for shallow-water equations based on FNO, U-Net and PINN. The latter required more than 10 minutes to be trained (20 times more than the OpInf-based model). It was not possible to directly compare the training time of the U-Net and FNO with the OpInf since these neural networks were constructed for 1,000 different

samples, while the OpInf, as well as the PINN, considered just one of them. For 1,000 samples, FNO and U-Net took more than 14,5 and 11,5 hours, respectively.

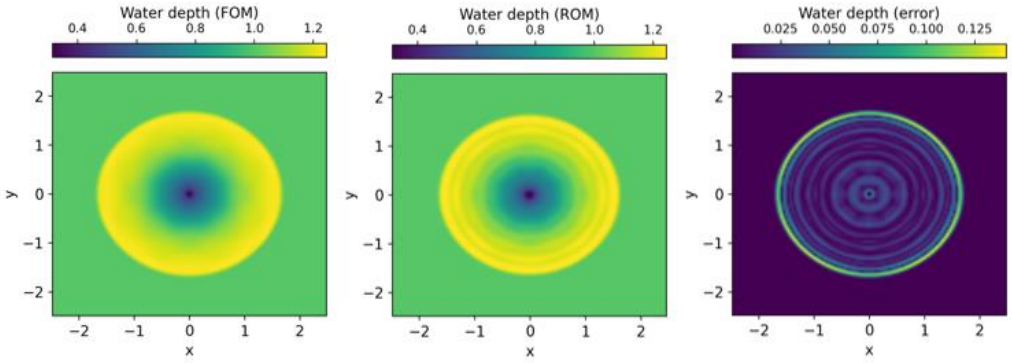

Figure 4. Spatial distribution of the water depth at the last training snapshot.

5. CONCLUSION

Scientific machine learning-based reduced-order models for the one-dimensional Burgers and the two-dimensional shallow-water equations were successfully built via the non-intrusive operator inference method. Few latent field variables were needed for approximating the full-space dynamics. Normalized root-mean-square errors at selected probe locations were not higher than 6.2 and 8.3% for Burgers and shallow-water cases, respectively. Similar performance was found at other locations. Regarding the convection-diffusion problem, 60% of the high-fidelity data were used to train the reduced model, demonstrating that a high amount of training data is not mandatory for the OpInf as it is for artificial neural networks. Moreover, for the shallow-water case, 25 seconds were required to build a surrogate model through OpInf, while physics-informed neural networks from literature took more than 10 minutes to accomplish the same task. Thus, the results show OpInf may be efficiently employed for model order reduction of fluid flow systems.

6. ACKNOWLEDGEMENTS

The authors would like to thank IBM Research Brazil and the Brazilian agencies CAPES and CNPq for the continuous support during the development of this research.

7. REFERENCES

Almeida, J.L.S., Pires, A.C., Cid, K.F.V., Nogueira Jr., A.C., 2022. “Non-intrusive operator inference for chaotic systems”, IEEE Transactions on Artificial Intelligence.

Brunton, S.L., Proctor, J.L., Kutz, J.N., 2016. “Discovering governing equations from data by sparse identification of nonlinear dynamical systems”, Proceedings of the National Academy of Sciences (PNAS), Vol. 113, no. 15, pp. 3932-3937.

Eivazi, H., Veisi, H., Naderi, M.H., Esfahanian, V., 2020. “Deep Neural Networks for Nonlinear Model Order Reduction of Unsteady Flows”, Physics of Fluids, Vol. 32, pp. 105104.

Kovachki, N., Lanthaler, S., Mishra, S., 2021. “On Universal Approximation and Error Bounds for Fourier Neural Operators”, Journal of Machine Learning Research, Vol. 22, pp. 1-76.

Lu, L., Jin, P., Pang, G., Zhang, Z., Karniadakis, G.E., 2021. “Learning nonlinear operators via DeepONet based on the universal approximation theorem of operators”, Nature Machine Intelligence, Vol. 3, pp. 218-229.

Lui, H.F.S., Wolf, W.R., 2019. “Construction of reduced-order models for fluid flows using deep feedforward neural networks”, Journal of Fluid Mechanics, Vol. 872, pp. 963-994.

McQuarrie, S.A., Huang, C., Willcox, K.E., 2021. “Data-driven reduced-order models via regularized Operator Inference for a single-injector combustion process”, Journal of the Royal Society of New Zealand, Vol. 51:2, pp. 194-211.

Pedregosa, F., Varoquax, G., Gramfort, A., Michel, V., Thirion, B., Grisel, O., Blondel, M., Prettenhofer, P., Weiss, R., Dubourg, V., Vanderplas, J., Passos, A., Cournapeau, D., Brucher, M., Perrot, M., Duchesnay, E., 2011. “Scikit-learn: Machine Learning in Python”, Journal of Machine Learning Research, Vol. 12, pp. 2825-2830.

Peherstorfer, B., Willcox, K., 2016. “Data-driven operator inference for nonintrusive projection-based model reduction”, Computer Methods in Applied Mechanics and Engineering, Vol. 306, pp. 196-215.

Qian, E., Kramer, B., Peherstorfer, B., Willcox, K., 2020. “Lift & Learn: Physics-informed machine learning for large-scale nonlinear dynamical systems”, Physica D, Vol. 406, pp. 132401.

Raissi, M., Perdikaris, P., Karniadakis, G.E., 2019. “Physics-informed neural networks: A deep learning framework for solving forward and inverse problems involving nonlinear partial differential equations”, Journal of Computational Physics, Vol. 378, pp. 686-707.

Rocha, P.R.B., Gomes, M.S.P., Almeida, J.L.S., Carvalho, A.M., Nogueira Jr., A.C., 2022. “Data-Driven Reduced-Order Model for Atmospheric CO2 Dispersion”. In AAAI 2022 Fall Symposium: The Role of AI in Responding to Climate Challenges, Arlington, Virginia, United States of America.

Rocha, P.R.B., Almeida, J.L.S., Gomes, M.S.P., Nogueira Jr., A.C., 2023. “Reduced-order modeling of the two-dimensional Rayleigh–Bénard convection flow through a non-intrusive operator inference”, Engineering Applications of Artificial Intelligence, Vol. 126(B), pp. 106923

Schmid, P.J., 2010. “Dynamic mode decomposition of numerical and experimental data”, Journal of Fluid Mechanics, Vol. 656, pp. 5-28.

Takamoto, M., Praditia, T., Leiteritz, R., MacKinlay, D., Alesiani, F., Pflüger, D., Niepert, M., 2023. “PDEBENCH: An Extensive Benchmark for Scientific Machine Learning”, arXiv:2210.07182.

Wang, Q., Hesthaven, J.S., Ray, D., 2019. “Non-intrusive reduced order modeling of unsteady flows using artificial neural networks with application to a combustion problem”, Journal of Computational Physics, Vol. 384, pp. 289-307.

Weiss, J., 2019. “A Tutorial on the Proper Orthogonal Decomposition”. In 2019 AIAA Aviation Forum, Dallas, Texas, United States of America.

Yu, J., Hesthaven, J.S., 2022. “Model order reduction for compressible flows solved using the discontinuous Galerkin methods”, Journal of Computational Physics, Vol. 468, pp. 111452.

8. RESPONSIBILITY NOTICE

The authors are the only responsible for the printed material included in this paper.